

Sonophotocatalytic Degradation Kinetics of an Azo Dye Amaranth

¹TUBA YETIM AND ²TANER TEKIN*

¹Faculty of Engineering, Department of Chemical Engineering, Erzurum Technical University, Erzurum, Turkey

²Faculty of Engineering, Department of Chemical Engineering, Atatürk University, 25240 Erzurum, Turkey
ttekin@atauni.edu.tr*

(Received on 7th April 2012, accepted in revised form 19th May 2012)

Summary: The effect of parameters such as initial concentration of dyestuff, light intensity, presence and the amplitude of ultrasound energy and temperature on sonophotocatalytic degradation kinetics of a monoazo dye amaranth (acid red 27-AR 27) was studied. The sonophotocatalytic degradation rate followed pseudo-first order kinetics with respect to amaranth concentrations. The ultrasound energy did not influence the activation energy. It was observed that the reaction rate accelerated in the presence of ultrasound energy during the experiments. A general equation was obtained for sonophotocatalytic degradation kinetics of amaranth which included the effect of ultrasound energy:

$$\left(\frac{-dC_{Dye}}{dt}\right) = 3,28 \cdot 10^{-7} (1 + 0,0471 W_U)^{0,151} \cdot \exp(-7965/T) \cdot I_a \left(\frac{4,38}{1 + 4,38(C_D)_0}\right)$$

Keywords: Textile dyes; Amaranth; Photocatalysis; Ultrasound; Degradation kinetics.

Introduction

Industrial dyestuffs and textile dyes constitute one of the largest groups of organic compounds that represent an increasing environmental danger. Fifteen percent of the total world production of dyes is lost during the dyeing process and is released in textile effluents. This situation often causes environmental problems. Physical (adsorption, ultrafiltration, reverse osmosis, coagulation, etc.) [1-3], biological (biodegradation) [4] and chemical methods (chlorination, ozonation) [5] are the most frequently used methods for removal of dyes from effluent water streams. But, these traditional processes for treatment of the effluents prove to be insufficient to purify the important quantity of waste waters after the different operations of textile dyeing and washing. Advanced oxidation processes (AOPs) are alternative methods for the complete degradation of dye. The usage of the advanced oxidation processes (AOPs) have improved during the last decade since they are able to eliminate the problem of dye destruction in aqueous systems. AOPs were based on the generation of very reactive species such as hydroxyl radicals ($\bullet\text{OH}$) that oxidize a broad range of pollutants quickly and non selectively. AOPs such as Fenton and photo-Fenton catalytic reactions [6,7], $\text{H}_2\text{O}_2/\text{UV}$ processes [8,9], photocatalysis and TiO_2 mediated photocatalysis [10-12], sonolysis and sonophotocatalysis [13-16] have been studied under a broad range of experimental conditions in order to reduce the color and organic load of dye containing effluent waste waters.

Photoexcitation of TiO_2 requires light with wavelengths of ≤ 380 nm. Upon absorption of a photon by TiO_2 , an electron is promoted to the conduction band, generating what is commonly

referred to as an electron-hole pair. The conduction band election is available for reduction and the valence band hole available for oxidation. The hole can subsequently react by electron transfer with a substrate to form a radical species or hydroxide (water) to form hydroxyl radical. In condensed oxygenated aqueous media, the surface of TiO_2 is completely hydroxylated and upon photoexcitation generates hydroxyl radical in an adsorbed state.

The hydroxyl radical is a powerful oxidizing agent and attacks organic compounds. Then intermediates (Int.) are formed. These intermediates react with hydroxyl radicals ($\text{OH}\cdot$) to produce final products (P), also hydroxyl radicals can be consumed by inactive species. The reaction rate follows pseudo-first order kinetics by considering the steady-state conditions and based on several other literature reports [17-19]. The kinetic expression is showed in the following form:

$$\left(\frac{-dC_D}{dt}\right) = k_p C_D \quad (1)$$

In this equation;

$$k_p = k_c I_a \left(\frac{K_D}{1 + K_D C_{D_0}}\right) \quad (2)$$

has been given [17].

Ultrasonic irradiation of aqueous solutions can result in the growth and collapse of gas bubbles (cavitation) producing high transient temperatures (up to 7.000 K in aqueous phase) and pressures (up to 1.000 atm), which leads to the formation of free radicals via the homolysis of water.

*To whom all correspondence should be addressed.



Ultrasonic irradiation has shown promise for the purification of contaminated water (or textile effluents) and involves at least in significant part standard hydroxyl radical mediated chain oxidation processes [20 and 21].

In the present work, the sonophotocatalytic degradation kinetics of monoazo textile dye acid red 27 was investigated. An empirical kinetic equation which contains the effect of ultrasound energy was obtained.

Results and Discussion

All of the parameters selected for this study (initial dye concentration, temperature, amplitude of ultrasound energy and light intensity) were studied with ultrasound energy (sonophotocatalytic) and without ultrasound energy (photocatalytic). The degradation results obtained from the initial dye concentrations are shown in Table-1 and temperatures in Table-2. From the experimental results, at initial concentration of 20 ppm in 30 minutes, the dye concentration decreases to 10.37 ppm or in other words a 48.1 % degradation is obtained in photocatalytic experiment. On the other hand, at the same conditions, the dye concentration decreases to 9.29 ppm and the degradation value approaches 53.6 % in sonophotocatalytic experiment. Also, at 313 K in 30 minutes the dye concentration decreases to 14.69 ppm from 30 ppm and a 51 % degradation value is obtained in photocatalytic experiment. Under the same conditions, the dye concentration decreases to 11.54 ppm from 30 ppm and a 61.5 % degradation is observed in sonophotocatalytic experiment. For the light intensity at 132 W/m² in 40 minutes, the dye concentration decreases to 10.43 ppm from 30 ppm or in other words, a 65.2 % degradation value was obtained in photocatalytic experiment. Under the same conditions, the dye concentration decreases to 8.91 ppm from 30 ppm and a 70.3 % degradation value is observed in sonophotocatalytic experiment. If the amplitude values are glanced, it can be seen that at 30 % amplitude the dye concentration decreases to 22.57 ppm from 30 ppm in 20 minutes and a 24.8 % degradation value is obtained. Under the same conditions, at 60 % amplitude the dye concentration value decreases to 17.11 ppm from 30 ppm and a 43 % degradation value is obtained. It is seen from the results the ultrasound energy accelerates the reaction rate.

When equation (1) for the degradation of dyestuffs is integrated;

$$\ln \left(\frac{C_{D0}}{C_D} \right) = k_p \cdot t \quad (4)$$

is obtained.

Time (t) versus $\ln(C_{D0}/C_D)$ plot is drawn for the obtained results with utilizing all of the parameters data by using the equation (4). The graphics without ultrasound and with ultrasound energy experiments for concentration are displayed in Fig. 1a. and Fig. 1b. A linear relation was obtained from the graphics for all parameters. This proves that the postulated kinetics model fits the experimental data and the reaction follows pseudo-first order kinetics. k_p values were calculated from the slope of these plots for all ultrasound and non-ultrasound energy experiments. They are listed in Table-3.

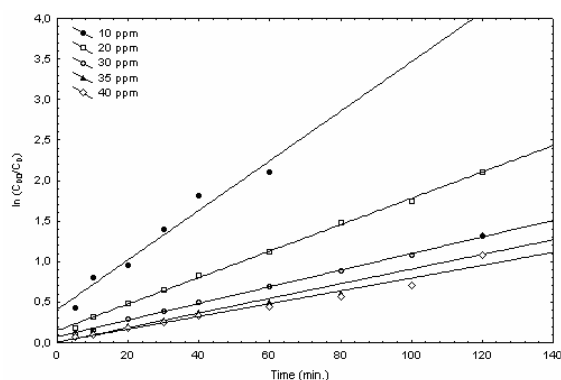


Fig. 1a: Plot of $\ln(C_{D0}/C_D)$ versus time without ultrasound with different initial concentrations.

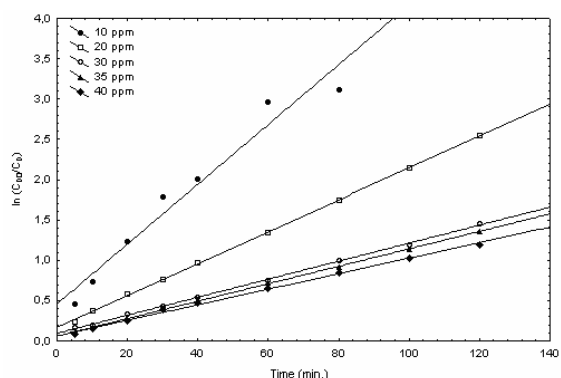


Fig. 1b: Plot of $\ln(C_{D0}/C_D)$ versus time with ultrasound with different initial concentrations.

Table-1: Degradation values for initial dye concentrations.

Time(min.)	Without Ultrasound (Photocatalytic)					With Ultrasound (Sonophotocatalytic)				
	Dye Concentration (ppm)					Dye Concentration (ppm)				
0	10	20	30	35	40	10	20	30	35	40
5	6.54	16.69	26.70	32.27	37.46	6.34	15.70	25.55	31.93	36.88
10	4.51	14.50	25.60	30.46	36.14	4.81	13.80	24.55	29.64	34.54
20	3.83	12.34	22.55	28.53	33.24	2.92	11.17	21.55	26.46	31.16
30	2.46	10.37	20.25	26.65	30.98	1.67	9.29	19.66	23.45	27.31
40	1.63	8.70	18.15	24.01	28.86	1.34	7.63	17.52	21.21	25.05
60	1.22	6.50	15.01	21.36	25.71	0.52	5.21	14.21	17.09	20.94
80	0.50	4.55	12.41	19.05	22.63	0.44	3.51	11.05	14.11	17.22
100	-	3.51	10.15	16.94	19.64	-	2.35	9.12	11.23	14.31
120	-	2.43	8.09	9.24	13.56	-	1.58	7.01	8.97	12.09

Table-2: Degradation values for various temperatures.

Temperature (K)	Without Ultrasound (Photocatalytic)				With Ultrasound (Sonophotocatalytic)			
	Dye Concentration (ppm)				Dye Concentration (ppm)			
293	303	313	323	293	303	313	323	
0	30	30	30	30	30	30	30	
5	27.69	26.70	25.91	23.20	27.23	25.55	22.60	21.49
10	26.85	25.60	22.63	18.55	26.05	24.55	19.11	16.90
15	26.21	23.88	20.45	14.84	25.31	22.57	17.04	14.03
20	25.20	22.55	18.46	11.30	24.47	21.55	15.05	9.75
25	24.71	21.53	16.07	8.74	23.81	20.19	12.94	7.82
30	24.18	20.25	14.69	6.60	23.12	19.66	11.54	5.41
35	23.20	19.07	12.31	4.69	22.27	18.54	9.55	3.78
40	22.79	18.15	11.35	3.14	21.31	17.52	7.84	2.55
45	22.06	17.05	9.40	2.50	20.95	16.47	6.30	1.84
50	21.50	15.94	8.14	1.85	20.20	15.22	4.99	1.35
60	20.87	15.01	7.00	0.84	19.33	14.21	3.91	0.67
80	17.88	12.41	3.88	-	17.07	11.05	1.34	-
100	17.20	10.15	1.78	-	15.58	9.12	-	-
120	15.83	8.09	-	-	13.95	7.01	-	-

Table-3: Measured and calculated (Eq.(8)) rate constants k_p for various dye concentrations, light intensities, temperatures and ultrasound powers.

Dye concentration (ppm)	Light intensity (W/m^2)	Temperature (K)	Ultrasound power (W)	k_p (min^{-1}) experimental	k_p (min^{-1}) theoretical
10	44	303	0	0.0306	0.0337
20	44	303	0	0.0163	0.0164
30	44	303	0	0.0102	0.0109
35	44	303	0	0.0090	0.0094
40	44	303	0	0.0079	0.0082
10	44	303	32.36	0.0371	0.0375
20	44	303	32.36	0.0197	0.0189
30	44	303	32.36	0.0111	0.0126
35	44	303	32.36	0.0108	0.0108
40	44	303	32.36	0.0096	0.0095
30	44	293	0	0.0050	0.0045
30	44	313	0	0.0272	0.0254
30	44	323	0	0.0600	0.0559
30	44	293	32.36	0.0058	0.0051
30	44	313	32.36	0.0363	0.0292
30	44	323	32.36	0.0644	0.0642
30	88	303	0	0.0229	0.0219
30	132	303	0	0.0348	0.0329
30	88	303	32.36	0.0290	0.0252
30	132	303	32.36	0.0377	0.0378
30	44	303	43.03	0.0127	0.0129
30	44	303	49.03	0.0130	0.0131
30	44	303	55.03	0.0135	0.0133

The Langmuir adsorption model is used for rate constant k_p is seen from the equation (2) [17]. k_p is inversely proportional with the initial dye concentration when the other parameters are constant.

$$k_p = k_1 \left(\frac{K_D}{1 + K_D (C_D)_0} \right) \quad (5)$$

When this equation is transformed to a straight-line equation (5) is obtained;

$$\frac{1}{k_p} = \frac{1}{k_1 K_D} + \frac{1}{k_1} C_{D_0} \quad (6)$$

$1/k_p$ versus concentration (C_{D_0}) plot is given in Fig. 2. for the ultrasound and non-ultrasound energy experiments of initial dye concentrations (10, 20, 30, 35 and 40 ppm). Intercept and slope of this curve is used for calculating the adsorption equilibrium constants (K_D). Calculated values of adsorption equilibrium constants are approximately the same with and without ultrasound energy: 4.37 and 4.39 l/mg. Also k_1 values with and without ultrasound energy are determined as 0.374 and 0.318 mg/(l.min.). It is seen from these results ultrasound energy did not caused any changes in the structure of dye. For this reason the equilibrium constants remained the same.

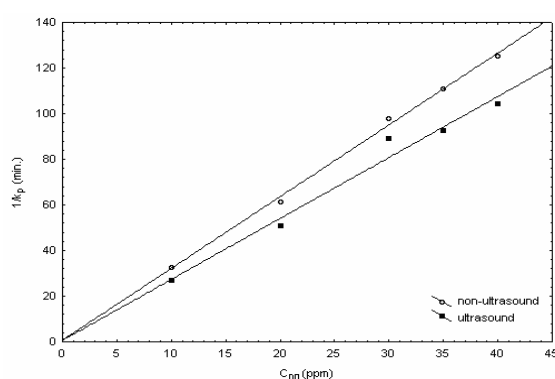


Fig. 2: Plot of $1/k_p$ versus initial concentration with and without ultrasound.

k_p changes linearly with light intensity (I_a) as seen from equation (2). Therefore when the various light intensities (44, 88, 132 W/m^2) versus k_p values is plotted (Fig. 3.) for the ultrasound and non-ultrasound energy experiments, the obtained linear curves show the accuracy of the model.

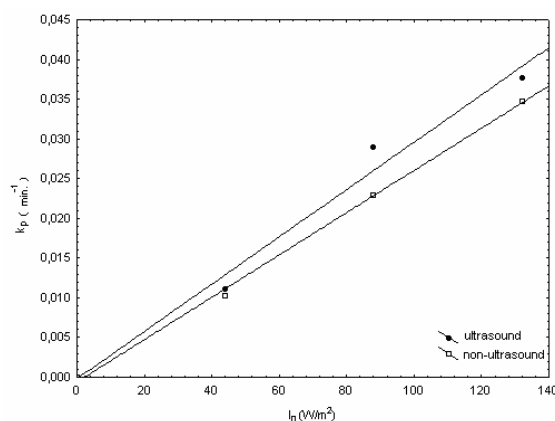


Fig. 3: Plot of k_p versus light intensity with and without ultrasound.

The activation energy of the reaction is estimated from the Arrhenius plot (Fig. 4.) as 66.3 kJ/mol from non-ultrasound energy experiments and 66.2 kJ/mol from ultrasound energy experiments. Thus, we conclude that the ultrasound energy did not influence the activation energy of the reaction.

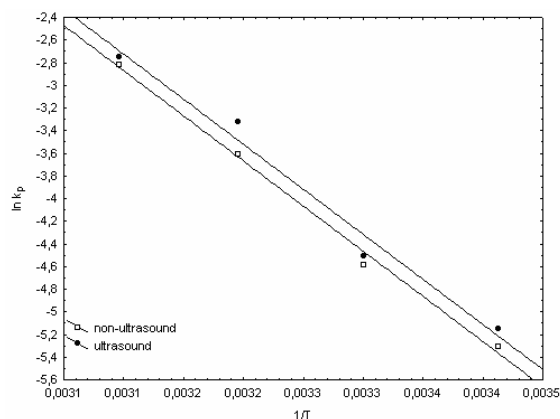


Fig. 4: Arrhenius plot.

The amplitude setting of the ultrasound generator was used to test the effect of the ultrasound power intensity on the degradation process. A linear dependence is obtained between amplitude setting and power input measured by calorimetric method [22]. For 20, 30, 40 and 50 % amplitude values the ultrasound powers are detected as 32.4, 43.0, 49.0 and 55.0W.

The dependence of reaction rate constant (k_p) on ultrasound power is usually expressed by the following relation [23-25];

$$k = A_0 (1 + bW_U)^c \exp(-E/RT) \quad (7)$$

Ultrasound energy does not effect the activation energy. If the equation (7) and equation (2) is combined, the reaction rate constant (k_p) will be as follows;

$$k_p = A_0 (1 + bW_U)^c \cdot \exp(-E/RT) \cdot I_a \left(\frac{K_D}{1 + K_D(C_D)_0} \right) \quad (8)$$

k_p values of different ultrasound powers, initial concentrations, light intensities and temperatures are used for nonlinear regression analysis. By calculating the non-linear regression analysis $A_0 = 3.28 \times 10^7$, $b = 0.0471$ and $c = 0.151$ values are obtained. Measured and calculated (from eq.(8)) rate constants (k_p) are given in Table-3. Measured rate constant values are plotted against the

calculated rate constant values in Fig. 5. It is seen from the Fig. 5. the fit between the values are very good.

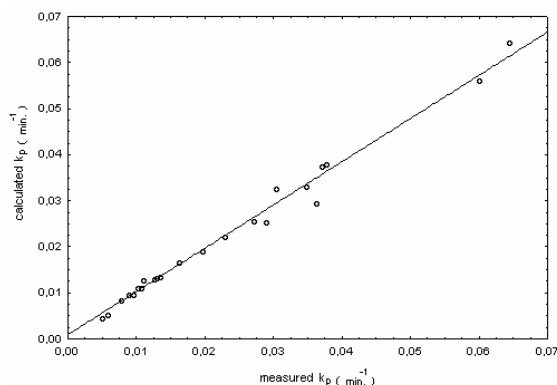


Fig. 5: Measured versus calculated k_p values.

There is an opinion about effect of ultrasound energy what the catalyst surface is cleaned by the ultrasound energy. It can make the catalyst more effective for chemical reactions. And there will be more reactions for producing the OH^\cdot radicals. After all OH^\cdot radical concentration will increase in the medium. The required OH^\cdot radicals will be obtained and the degradation will be much more and fast. Thus the reaction time will be reduced by this method.

Experimental

A schematic illustration of the experimental set-up is shown in Fig. 6. It consists of an ultrasonic generator (Type Cole Parmer, Ultrasonic homogenizer, 750 W, 20 kHz) together with a probe. Pen-Ray UV lamp (Cole, Parmer, 254 nm, 44 W/m^2) was used as the radiation source. In the experiments for investigating the effect of light intensity, the irradiations were carried out using firstly one UV lamp, then two UV lamps and the last three UV lamps. The reaction temperature was controlled by circulation of water at the desired temperature through the jacket. Air was blown into the reaction medium by an air pump in a constant flow to maintain the solution saturated with oxygen during the course of the reaction.

Procedure

The employed photocatalyst was commercial titanium dioxide supplied by Degussa (P25). According to the manufacturer's specifications, P25 has an elementary particle size of 30 nm, a BET specific surface area of 50 m^2/g . Amaranth (acid red

27) was obtained from Rasih Celik Textile Company (Turkey) and was used without further purification.

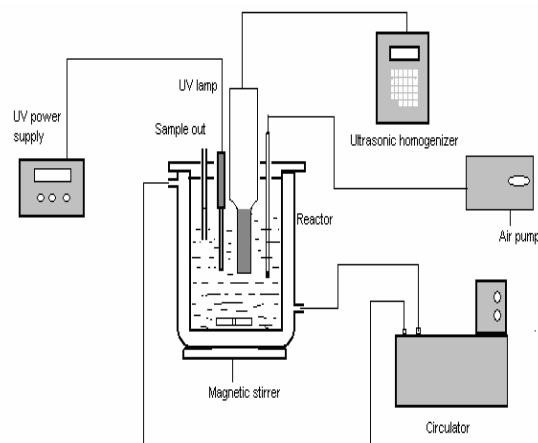


Fig. 6: Schematic illustration of sonophotocatalytic system.

The experiments were carried out with 300 ml dye solutions prepared in appropriate concentrations using deionized water. 30, 40, 50, 60 % amplitude of ultrasound energy and 20, 30, 40, 50 $^\circ\text{C}$ (± 0.4 $^\circ\text{C}$) temperatures were used for the experiments. Air was blown into the reaction medium by an air pump in a constant flow, to maintain the solution saturated with oxygen during the reaction. For the light intensity the pen-ray UV lamps were used and the parameters were determined as 44, 88 and 132 W/m^2 . Different concentrations of dye solutions (10, 20, 30, 35 and 40 ppm) and 500 mg/l TiO_2 were introduced in this reactor. Suspensions of 5 ml were withdrawn at regular intervals and were immediately centrifuged at 6000 rpm for 10 min to completely remove catalyst particles. For the progress of photocatalytic degradation, dye concentration analyzed by measuring the absorbance of the solution samples with UV-Vis spectro-photometer (Thermo Electron Evolution 500 spectrophotometer) at $\lambda_{\text{max}} = 522$ nm. All experiments were repeated with ultrasound and non-ultrasound energy for displaying the effect of ultrasound energy while the effect of parameters was investigated.

Conclusions

1. From the experimental results, we obtained that the sonophotocatalytic degradation rate followed pseudo-first order kinetics.
2. Measured rate constant values were plotted against the calculated rate constant values and the fitness was very good.
3. We concluded that the ultrasound energy did not influence the activation energy of the reaction. It

was seen that the ultrasound energy was effective on the reaction rate constant (k_p).

4. A general equation was obtained for sonophotocatalytic degradation kinetics of monoazo dye acid red 27 which included the effect of ultrasound energy.

$$\left(\frac{-dC_{Dye}}{dt}\right) = 3,28 \cdot 10^7 (1 + 0,0471W_U)^{0,151} \cdot \exp(-7965/T) \cdot I_a \left(\frac{4,38}{1 + 4,38(C_D)_0}\right) \quad (9)$$

1. It was observed that the ultrasound energy increased the degradation of dyestuffs. The OH⁻ radicals obtained from both sonolysis and photocatalysis thus, the number of OH⁻ radicals were increased. Therefore, the degradation rate increased much more.
2. This process provided to reduce reaction time.
3. Using the sonolysis and photocatalysis simultaneously can be more effective to remove the dyestuffs from the wastewater because of synergistic effect between photocatalysis and sonolysis.

Acknowledgements

This study is part of research project supported by TUBITAK, project number is 105T258. The authors thank Prof.Dr. Deniz Uner (Middle East Technical University/Turkey) for useful discussions.

References

1. W. Z. Tang and H. An, *Chemosphere*, **31**, 4171 (1995).
2. W. S. Kuo and P. H. Ho, *Chemosphere*, **45**, 77 (2001).
3. C. Galindo, P. Jacques and A. Kalt, *Chemosphere*, **45**, 997 (2001).
4. U. U. Jadhav, V. V. Dawkar, G. S. Ghodake and S. P. Govindwar, *Journal of Hazardous Materials*, **158**, 507 (2008).
5. S. M. Burkinshaw and O. Kabambe, *Dyes Pigments*, **83**, 363 (2009).
6. M. Tokumura, H. T. Znad and Y. Kawase, *Chemical Engineering Science*, **61**, 6361 (2006).
7. S. F. Kang, C. H. Liao, S. T. Po, *Chemosphere*, **41**, 1287 (2000).
8. U. Bali, E. Catalkaya and F. Şengul, *Journal of Hazardous Materials*, **114**, 159 (2004).
9. U. G. Akpan and B. H. Hameed, *Journal of Hazardous Materials*, **170**, 520 (2009).
10. S. K. Kansal, M. Singh and D. Sud, *Journal of Hazardous Materials*, **141**, 581 (2007).
11. M. Abbasi and N. R. Asl, *Journal of Hazardous Materials*, **153**, 942 (2008).
12. J. P. Lorimer, T. J. Mason, M. Plattes and S. S. Phull, *Ultrasonics Sonochemistry*, **7**, 237 (2000).
13. C. G. Joseph, G. Li Puma, A. Bono and D. Krishnaiah, *Ultrasonics Sonochemistry*, **16**, 583 (2009).
14. S. Toma, A. Gaplovsky and J. L. Luche, *Ultrasonics Sonochemistry*, **8**, 201 (2001).
15. N. Daneshvar, M. Rabbani, N. Modirshahla and M. A. Behnajady, *Journal of Photochemistry and Photobiology A: Chemistry*, **168**, 39 (2004).
16. R. Terzian and N. Serpone, *Journal of Photochemistry and Photobiology A: Chemistry*, **89**, 163 (1995).
17. I. K. Konstantinou and T. A. Albanis, *Applied Catalysis B: Environmental*, **49**, 1 (2004).
18. L. A. Crum, T. J. Mason, J. L. Reisse and K. S. Suslick, *Sonochemistry and Sonoluminescence*, Kluwer Academic, Dordrecht, (1999).
19. T. J. Mason and P. J. Lorimer, *Sonochemistry: Theory, Applications and Uses of ultrasound in Chemistry*, Ellis Horwood (1989).
20. T. Kimura, T. Sakamoto, J. Leveque, H. Sohmiya, M. Fujita, S. Ikeda and T. Ando, *Ultrasonics Sonochemistry*, **3**, 157 (1996).
21. C. Horst, Y. S. Chen, U. Kunz and U. Hoffmann, *Chemical Engineering Science*, **51**, 1837 (1996).
22. T. Tekin, D. Tekin and M. Bayramoglu, *Ultrasonics Sonochemistry*, **8**, 373 (2001).
23. T. Ingeç and T. Tekin, *Chemical Engineering Technology*, **27**, 150 (2004).